Cell Reports, Volume *29*

Supplemental Information

Intra-Vκ Cluster Recombination Shapes the Ig Kappa Locus Repertoire

Kenta Shinoda, Yaakov Maman, Andres Canela, David G. Schatz, Ferenc Livak, and André Nussenzweig

Figure S1

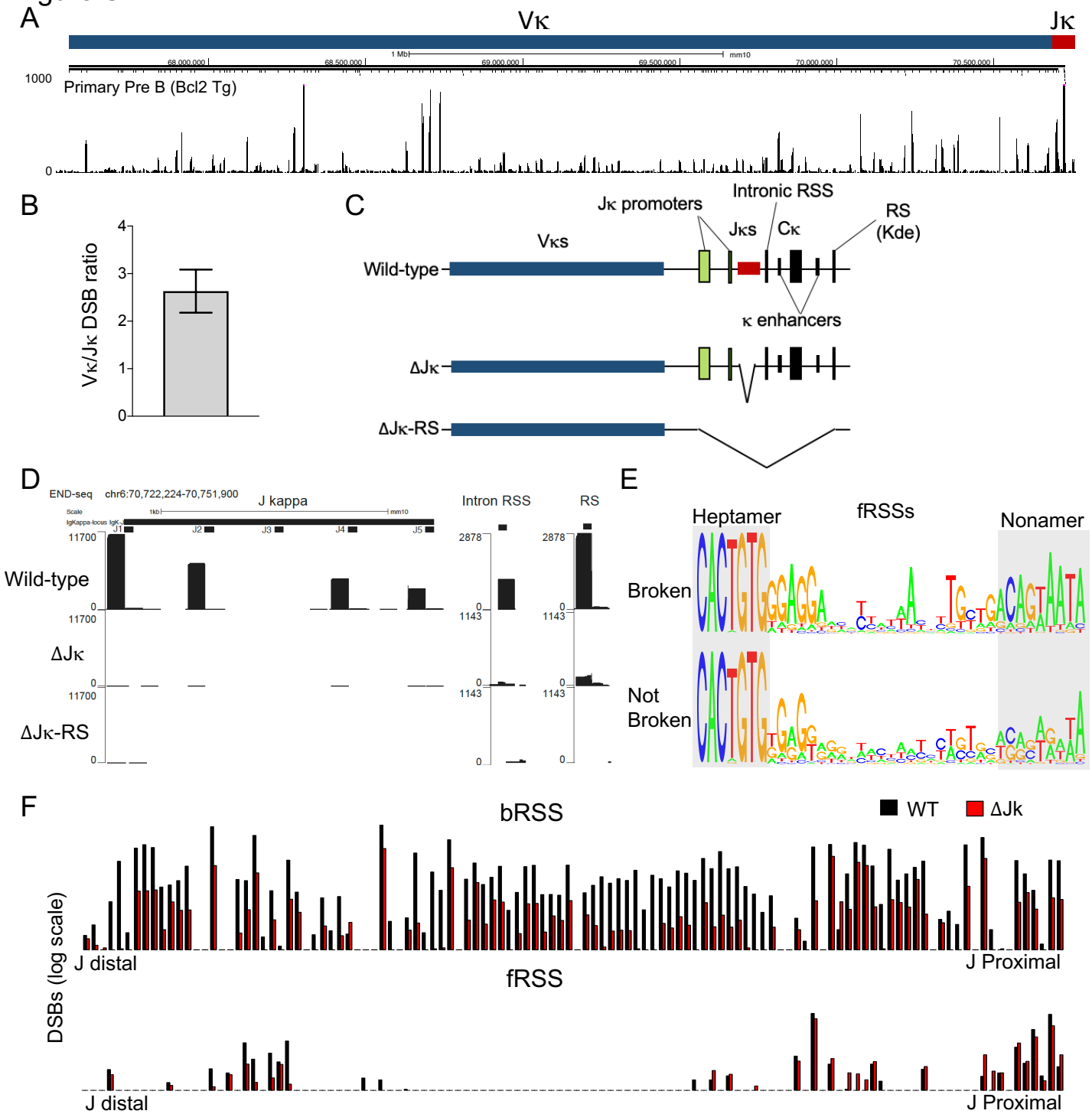

Figure S1. Vκ DSBs occur independently of Jκ or the Jκ-associated recombination center. Related to Figure 1

(A) END-seq reads at the Igκ locus from *ex vivo* cultured VavP-Bcl2-transgenic, primary mouse bone marrow pre-B cells. **(B)** Ratio of total DSB frequency in the Vκ region compared to Jk region detected by END-seq in v-Abl cells. Error bar represent standard error of seven independent experiments. **(C)** Schematic diagram of the genomic organization of the Igκ locus in WT (top row), ΔJκ (middle row) and ΔJκ-RS (bottom row) genotypes. **(D)** END-seq tracks around the Jκ-RS regions from WT (top row), ΔJκ (middle row) and ΔJκ-RS (bottom row) v-Abl-transformed pre-B cells**. (E)** Consensus sequence logo at the broken (top) and non broken (bottom) fRSSs of Vκ region, as detected by END-seq in WT v-Abl-transformed pre-B cells. Heptamer and nonamer sequences are highlighted in grey. **(F)** DSB levels of individual Vκ bRSS (top) and fRSS (bottom) in WT(black) and ΔJk (red) v-Abl-transformed pre-B cells, as measured by END-seq.

Figure S2

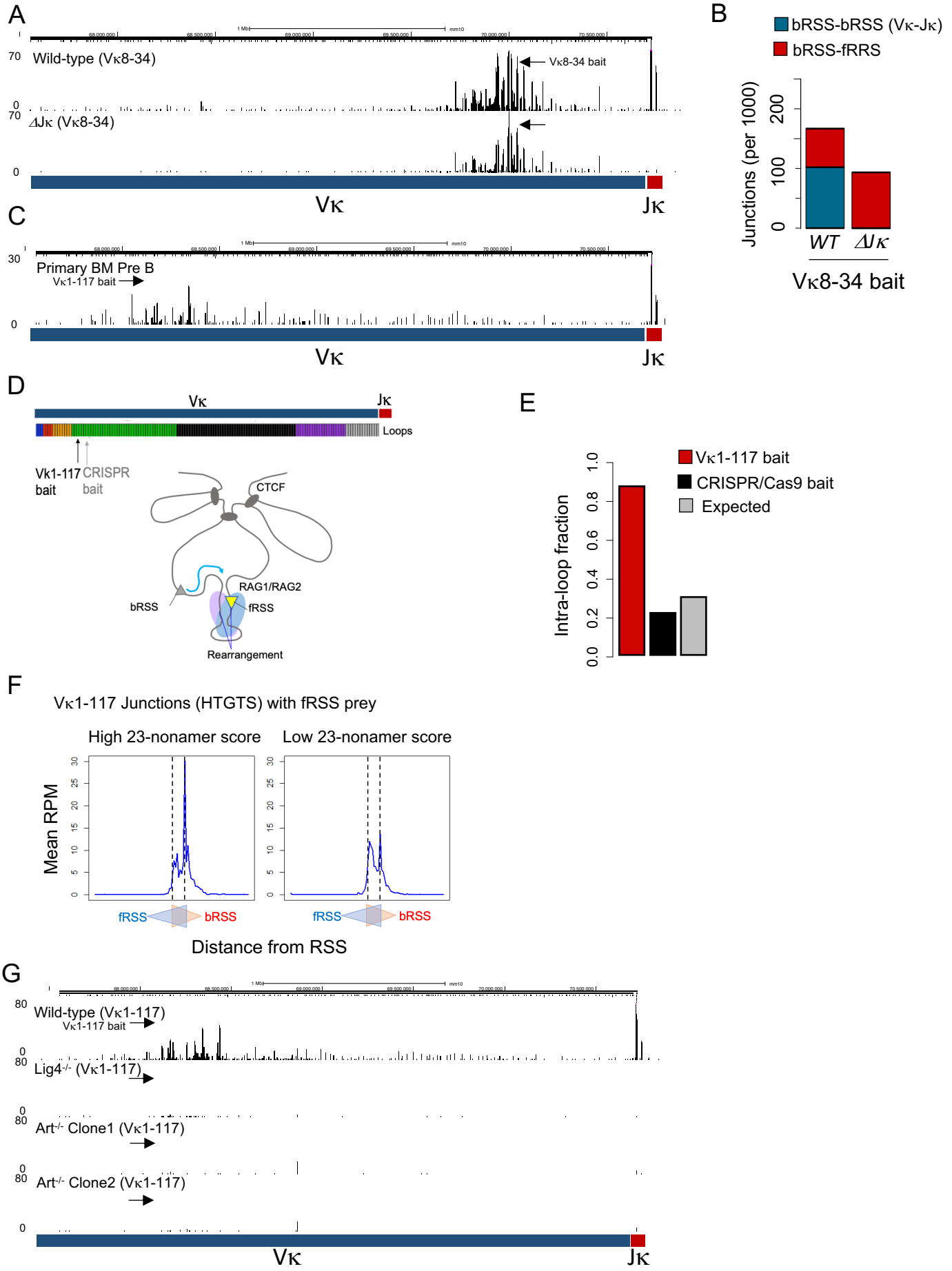
A
Wild-type (Vκ8-34)
Vκ8-34 bait
ΔJκ (Vκ8-34)
Vκ
Jκ
B
bRSS-bRSS (Vκ-Jκ)
bRSS-fRRS
Junctions (per 1000)
WT
ΔJκ
Vκ8-34 bait
C
Primary BM Pre B
Vκ1-117 bait
Vκ
Jκ
D
Vκ
Jκ
Loops
Vk1-117 bait
CRISPR bait
CTCF
RAG1/RAG2
bRSS
fRSS
Rearrangement
E
Vκ1-117 bait
CRISPR/Cas9 bait
Expected
Intra-loop fraction
F
Vκ1-117 Junctions (HTGTS) with fRSS prey
High 23-nonamer score
Low 23-nonamer score
Mean RPM
fRSS
bRSS
Distance from RSS
G
Wild-type (Vκ1-117)
Vκ1-117 bait
Lig4-/- (Vκ1-117)
Art-/- Clone1 (Vκ1-117)
Art-/- Clone2 (Vκ1-117)
Vκ
Jκ

Figure S2. Frequent fRSS mediated intra-Vκ cluster rearrangements within loop domains. Related to Figure 2.

(A) HTGTS junction profiles of WT (top) and ΔJκ (bottom) v-Abl-transformed pre-B cells (Vκ8-34 bait). Arrow indicates the approximate position of the bait primer. **(B)** The number of junctions (per 1000 total junctions) of bRSS-bRSS (Vκ-Jκ in blue) and bRSS-fRSS (intra-Vκ in red) recombinations in v-Abl-transformed pre-B cells (WT and ΔJκ) detected using the Vκ8-34 bait. **(C)** HTGTS junction profiles of WT primary, mouse bone marrow pre-B cells with Vκ1-117 bait. Arrow indicates the approximate position of the bait primer. **(D)** Top: Schematic diagram of Vκ chromosomal loops (Karki et al., 2018). The positions of the Vκ1-117 and CRISPR/Cas9 baits are indicated. Bottom: Cartoon representation of RAG1/2 scanning within a loop to engage fRSS and bRSS. **(E)** Fraction of junctions obtained with Vκ1-117 (red) and CRISPR/Cas9 (black) baits that reside within the same loop as the bait (loop marked in green in panel d). Grey bar represents the expected fraction of intra-loop junctions derived from the proportion of RSS that reside within this loop. **(F)** Aggregate plot of junctions associated with the Vκ1-117 bait in WT v-Abl-transformed pre-B. Vκ fRSS of high PWM score (left panel) and low PWM score (right panel) are shown separately. The first nucleotide of bRSS and fRSS are depicted by two overlapping triangles. The relatively high fraction of junctions at the bRSS of prey Vκ genes could be the result of secondary rearrangements, possibly hybrid joints, which disappear in the ΔJκ clone (see Figure 2C). **(G)** HTGTS junction profiles from WT, *Lig4*$^{-/-}$, *Artemis*$^{-/-}$ clone 1, and *Artemis*$^{-/-}$ clone 2 v-Abl-transformed pre-B cells detected with the Vκ1-117 bait. Arrow indicates the approximate position of the Vκ1-117 bait primer.

Figure S3

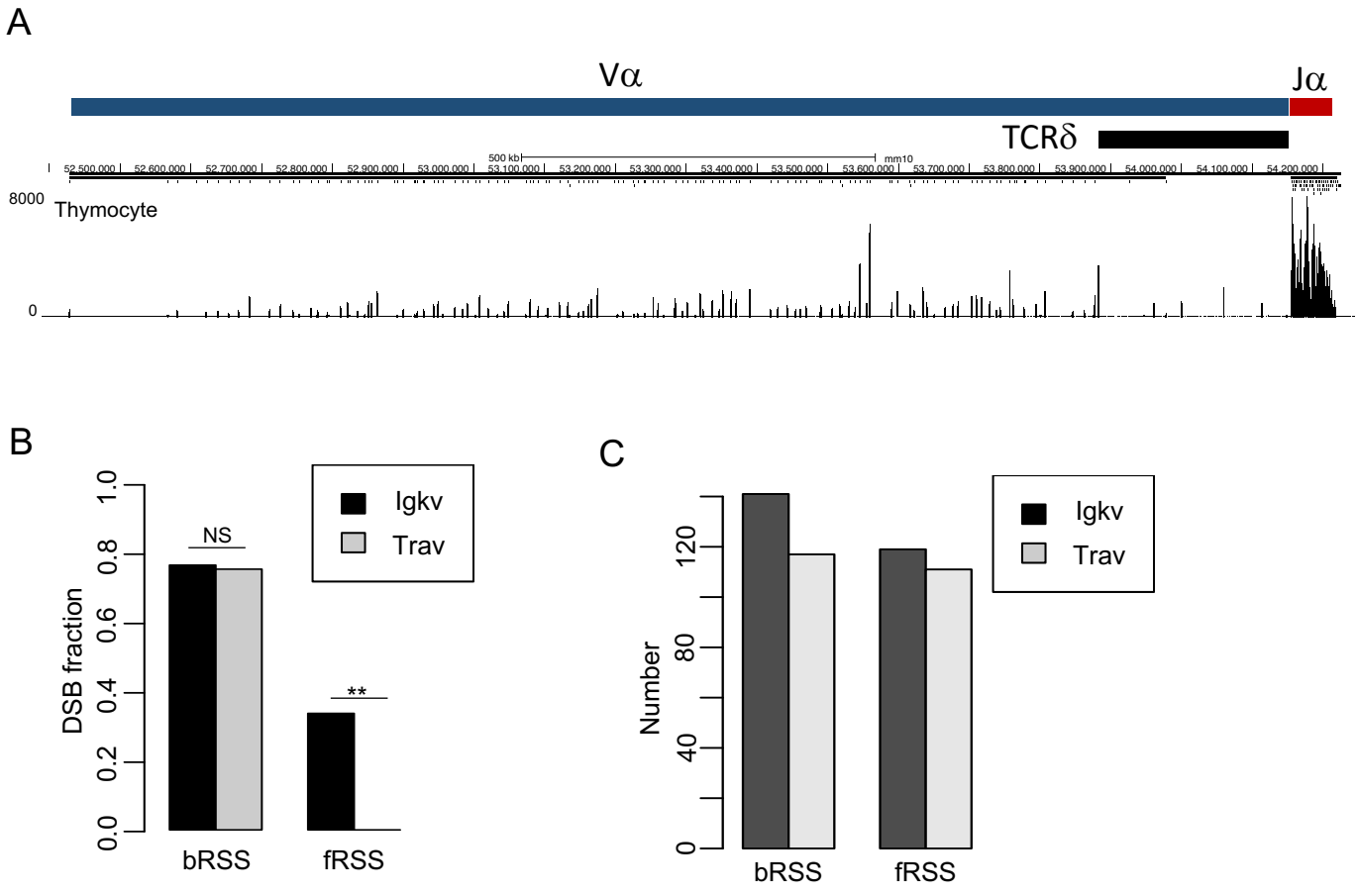

Figure S3. Distribution of bRSS and fRSS breakage within the Igκ and TCRα loci. Related to Figure 3. **(A)** END-seq tracks at the TCRα/δ locus from WT DP mouse thymocytes. **(B)** Fraction of cleaved bRSS and cleaved potential fRSS (here defined as palindromic heptamer of an RSS) within all Vκ (black) and Vα (grey) gene segments, as detected by END-seq. NS $p > 0.05$, **$p < 1e^{-10}$, fisher test. **(C)** There are similar number of V genes with bRSS and with potential fRSS (palindromic heptamer) in the Igκ (black) and TCRα (grey) loci.

Figure S4

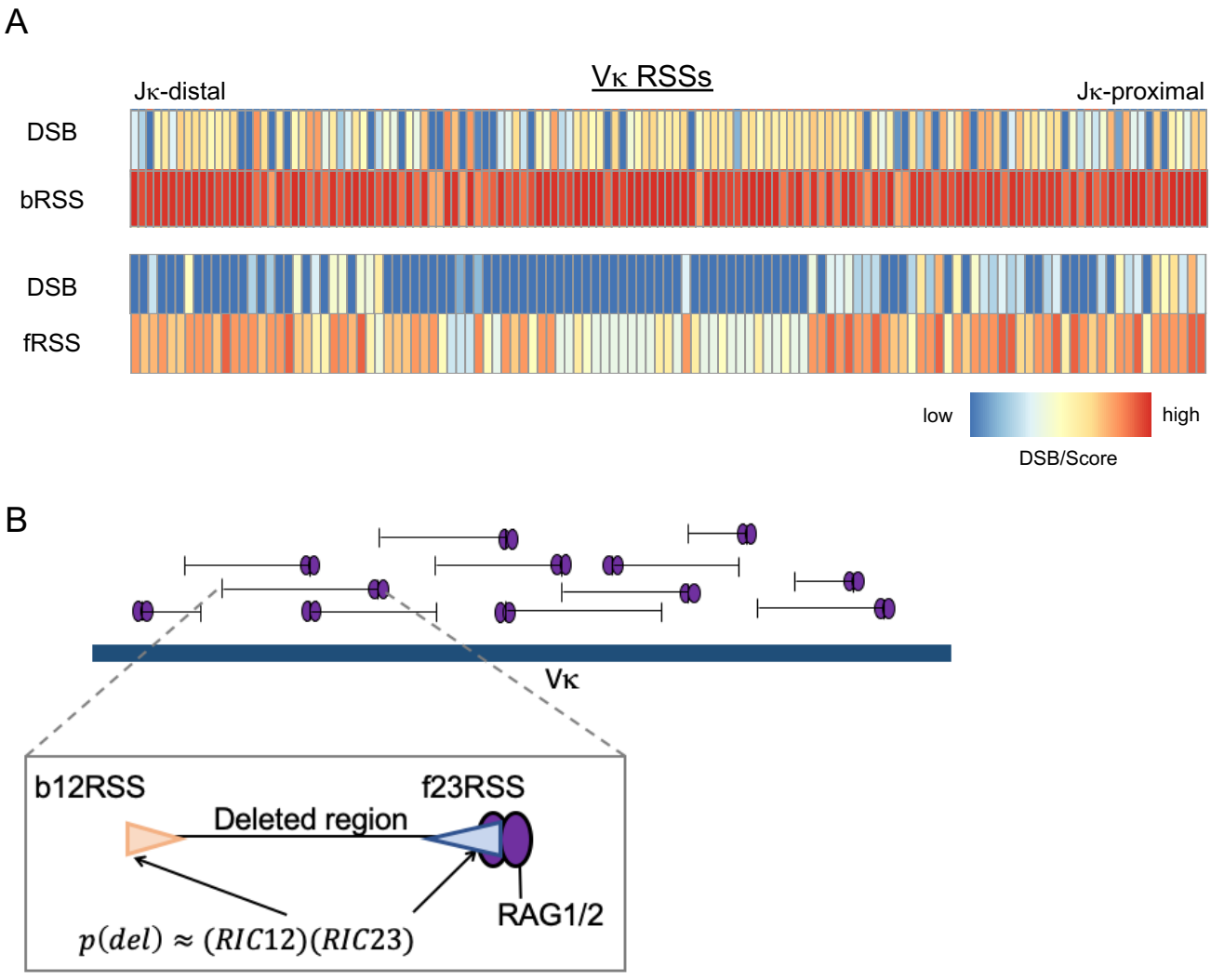

Figure S4. DSB distribution and probability of Vκ segment deletion. Related to Figure 5.
(A) Heatmap of DSB signal (upper) and PWM score (bottom) of 12mer bRSS or 23mer -fRSS within the Vκ cluster. Each box corresponds to the RSS of a Vκ gene and the color indicates the strength of DSB signal or the PWM score of the RSS. **(B)** The probability of a Vκ gene segment deletion is estimated by the combined probability of (i) the functional quality of the pair of bRSS and fRSS as measured with RIC score, (ii) RAG binding to at least one of the two RSS within the pairs, and (iii) loop coefficient (see Methods for details).

Table S1

gRNAs used to generate mutant v-Abl cell lines	
ΔJk up (gRNA)	AAGCATGCGTGGAAGCGCTT
ΔJk down (gRNA)	GGGCTCATTATCAGTTGACG
ΔJk-RS up (gRNA)	ATCACACGTATAGAGTAAGC
ΔJk-RS down (gRNA)	CCTGCCCACACGACTCCTTC
Primers used for screening of gene deletion	
ΔJk-Fw	ACTAACTGCTGAGCCACCTC
ΔJk-Rv	GCAGTCAGACCCAGATCTCAA
ΔJk-intact-Rv	AGCCACAGACATAGACAACGG
ΔJk-RS-Fw	ACCTGGGGAACAAAACTGGA
ΔJk-RS-Rv	AATCTGCCTGTCTGAAGCCC
ΔJk-RS-intact-Rv	GGAAGACAAAGGAGGCCACG
sgRNA targeted to downstream of Vk1-117	
Vk1-117 CRISPR-Cas9	TTGCTACATATCTGGCACCG
Primers and adaptors used for HTGTS	
Adaptor-upper	GGTACACGACGCTCTTCCGATCTNNNNNN/3AmMO/
Adaptor-lower	/5Phos/AGATCGGAAGAGCGTCGTGTACC/3AmMO/
I5-bridge	AATGATACGGCGACCACCGAGATCTACACTCTTTCCCTACACGACGCTCTTCCGATC∗T
P5-I5c	AATGATACGGCGACCACCGAGATCTACACTCTTT∗C
P7-I7c	CAAGCAGAAGACGGCATACGAGATCGGTCTCGGCATTCCTGCTGAACCGCTCTT∗C
Jk1-bio	/5Biosg/TTCCCAGCTTTGCTTACGGAG
I7-Jk1-nested-barcode1	CTCGGCATTCCTGCTGAACCGCTCTTCCGATCTATTACTCGAGTGCCAGAATCTGGTTTCAGAG
Vk1-117-bio	/5Biosg/CAGAAGCCTTCAGTATGCACCA
I7-Vk1-117-nested-barcode1	CTCGGCATTCCTGCTGAACCGCTCTTCCGATCTATTACTCGCAGGGACAGATTTCACACTCAAG
I7-Vk1-117-nested-barcode2	CTCGGCATTCCTGCTGAACCGCTCTTCCGATCTTCCGGAGACAGGGACAGATTTCACACTCAAG
I7-Vk1-117-nested-barcode3	CTCGGCATTCCTGCTGAACCGCTCTTCCGATCTCGCTCATTCAGGGACAGATTTCACACTCAAG
I7-Vk1-117-nested-barcode4	CTCGGCATTCCTGCTGAACCGCTCTTCCGATCTGAGATTCCCAGGGACAGATTTCACACTCAAG
Vk8-34-bio	/5Biosg/CAGAAACCAGGACGATCTCCT
I7-Vk8-34-nested-barcode7	CTCGGCATTCCTGCTGAACCGCTCTTCCGATCTCTGAAGCTACTAGGGTATCTGGAGTCCCTG
I7-Vk8-34-nested-barcode8	CTCGGCATTCCTGCTGAACCGCTCTTCCGATCTTAATGCGCACTAGGGTATCTGGAGTCCCTG
Bio-Vk1-117-CRISPR	/5Biosg/TATGAACAGGTGCCCTCCCA
I7-Vk1-117-CRISPR-barcode10	CTCGGCATTCCTGCTGAACCGCTCTTCCGATCTTCCGCGAACCTCCTCCGACCCACTACTG
bio-human-IGJK1	/5Biosg/TCCCCAGGACATTTCTGAAG
I7-human-IGJK1-barcode1	CTCGGCATTCCTGCTGAACCGCTCTTCCGATCTATTACTCGGGCTGATTGCAGAGTCACCT
bio-human-IGVK2-28	/5Biosg/TAACTTTGCAATTCATTATTTCAGGA
I7-human-IGVK2-28-barcode4	CTCGGCATTCCTGCTGAACCGCTCTTCCGATCTGAGATTCCTGGATACAACTATTTGGATTGG
bio-human-IGVK3-20	/5Biosg/GCACCCTGTCTTTGTCTCCA
I7-human-IGVK3-20-barcode7	CTCGGCATTCCTGCTGAACCGCTCTTCCGATCTCTGAAGCTATCAGCAGACTGGAGCCTGAA

*Phosphorothioate bonds, /5Biosg/: 5' Biotin, /3AmMO/: 3' Amino modifier

Table S1. List of Oligos. Related to STAR Methods.